THE JOURNAL OF PHYSICAL CHEMISTRY C

Article

pubs.acs.org/JPCC

Nanometer-Wide Lines of Self-Assembled Monolayer: A Molecular Dynamics Simulation Study

Joyanta K. Saha, Hyojeong Kim, and Joonkyung Jang*

Department of Nanomaterials Engineering, Pusan National University, Miryang 627-706 Republic of Korea

ABSTRACT: A molecular dynamics simulation was performed to study the nanometer-wide lines carved out of a self-assembled monolayer (SAM) of octadecanethiol on gold. This simulation is relevant to the nanoscale SAM patterns created by nanolithography. The molecular packing structure in the SAM line was compared with that in a bulk SAM. A stable SAM line must be at least 1.7 nm wide, and two lines can merge if they are less than 3.0 nm apart. This presumably sets the ultimate resolution of SAM patterns. A finite length of the SAM line or the crossing of two lines further destabilizes the SAM line.

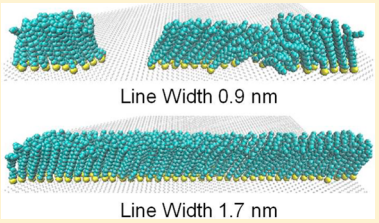

I. INTRODUCTION

Self-assembled monolayers (SAMs) are used in molecular electronics, biosensors, and nanofabrication, to name a few.[1−3] In particular, the SAMs of alkanethiols have been used extensively for tailoring the interfacial properties of metal and semiconductor surfaces because of their stable and well-defined structures.[2,1] In the SAM of alkanethiol on a gold (111) surface, the adsorbed sulfur atoms develop a $\sqrt{3} \times \sqrt{3}$R30° overlayer (according to Wood's notation[4]), and the alkyl chains of the molecules are tilted slightly (∼30°) from the surface normal.[1] The stability of the SAM originates from both the strong adhesion of sulfur atoms to the surface and the near parallel packing of the alkyl chains of thiol molecules.

The SAM patterns with nanometer resolution are generated routinely using a range of lithographic techniques. For example, dip-pen nanolithography (DPN)[5,6] and microcontact printing[7,8] utilize a spatially narrow transfer of molecules from an atomic force microscope (AFM) tip and a stamp, respectively. Nanografting,[9] photolithography,[10] nanoimprinting,[11] and interferometric lithography[12] are also used to produce nanometere-sized SAM patterns. Thus far, a SAM line as narrow as 15 nm in width has been patterned on a gold surface.[13] Parallel SAM lines as close as 5 nm apart have been fabricated.

As nanotechnology develops further, SAM patterns with even finer resolutions are expected to appear. Given a SAM pattern will be destabilized as its size decreases to a few nanometers in width, the question is how narrow these SAM patterns can be. Moreover, these finite-sized SAM patterns can have new structural features compared to those of the bulk SAM. Currently, the properties of nanoscale SAMs are not well understood, which is in contrast to those of bulk SAMs. In this viewpoint, nanometer-sized circular SAM islands were recently investigated by molecular dynamics (MD) simulations.[14,15] A circular SAM island was found to become unstable if its diameter is less than 1.9 nm. In addition, the tilt direction of each alkyl chain constituting a circular SAM island rotates clockwise or counterclockwise around the center of the SAM island.

This study investigated another common motif of SAM patterns: a nanometer-wide line made from octadecanthiol molecules on a gold surface. MD simulations were used to estimate the minimum width of a stable SAM line, which sets the ultimate resolution of a SAM pattern. This study also examined how close two SAM patterns can approach each other without coalescence, which is related to the spatial resolution of the SAM patterns that can be fabricated. Also examined are other line-based patterns, such as crosses. The novel features of the molecular packing structure of the SAM line are reported.

II. SIMULATION DETAILS

The SAM patterns of 1-octadecanethiol ($SH(CH_2)_{17}CH_3$, ODT) molecules on a gold (111) surface were simulated. This molecule is the prototypical molecule used in DPN and microcontact printing. The gold surface was modeled as a slab made from two layers and 12 800 atoms. The CH_3, CH_2, and SH groups of ODT were treated as united atoms (only H atoms were implicit).[16,17] Nine united atoms of CH_3 or CH_2, which have odd (1−17) numbers of intervening CH_2 groups between them, and the S atom were selected to define the *tilt direction* vector $\vec{u}_i$ of each molecule, *i*. $\vec{u}_i$ was defined as the average of the direction vectors from the S atom to these united atoms (Figure 1).[18,17] The *tilt angle*, θ_i, of the *i*th molecule is given by the polar angle of $\vec{u}_i$ from the surface normal (which lies along the *Z* axis). The surface projection of $\vec{u}_i$ was designated $\vec{v}_i$. The backbone plane orientation of the ODT molecule is described by the vector

$$\vec{b}_i = \sum_{j=1}^{15} (-1)^j \vec{r}_j \qquad (1)$$

where $\vec{r}_j$ is the *j*th C−C bond vector starting from the S atom. In eq 1, three methyl groups at the tail of the chain (*j* = 17, 18,

Received: October 9, 2012
Revised: November 17, 2012
Published: November 27, 2012

dx.doi.org/10.1021/jp3099736 | *J. Phys. Chem. C* 2012, 116, 25928−25933

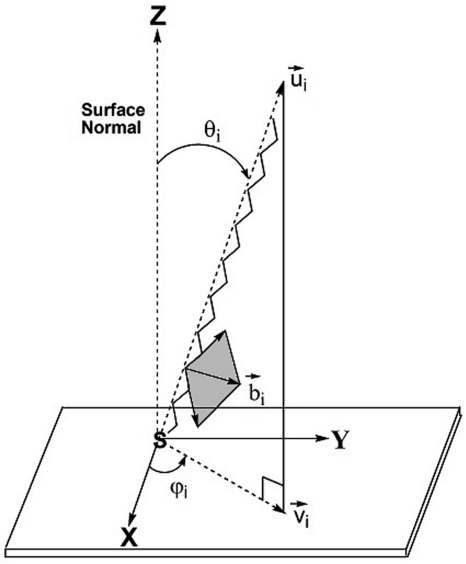

Figure 1. Orientation of an ODT molecule on a gold surface. Shown is an ODT molecule with all-trans conformations. To define the tilt direction vector $\vec{u}_i$ for each molecule, i, nine CH_3 or CH_2 groups, which have odd (1−17) numbers of intervening CH_2 groups between them, and the S atom were selected. $\vec{u}_i$ is defined as the average of the direction vectors from the S atom to these selected united atoms. $\vec{v}_i$ is defined as the surface (XY plane) projection of $\vec{u}_i$. The tilt angle θ_i is the polar angle of $\vec{u}_i$ measured from the surface normal (Z direction). φ_i is the azimuthal angle of $\vec{u}_i$.

19) were excluded because they contain many gauche defects. Physically, $\vec{b}_i$ is the average of the vectors that dissect the C−C−C or C−C−S angle and lie on the planes defined by these triplets (the shaded plane in Figure 1). $\vec{u}_i$, $\vec{v}_i$ and $\vec{b}_i$ were normalized as unit vectors. The molecular orientation of the SAM line was quantified by examining the order parameter[19]

$$O_X = \langle 0.5[(\vec{X}_i \cdot \vec{X}_j)^2 - 1] \rangle_{i \neq j} \quad (2)$$

where $\langle \rangle_{i \neq j}$ represents the average over all intermolecular pairs and $\vec{X}_i = \vec{u}_i$ or $\vec{b}_i$.

The bond stretching and bending angle interactions between the united atoms were modeled using the harmonic potentials.[20] The four-atom torsion potential (C−C−C−C or C−C−C−S) takes a triple cosine function of the dihedral angle ϕ, where $\phi = \pm 180°$ and $\phi = \pm 60°$ correspond to the trans and gauche conformations, respectively.[21] All nonbonded interatomic pair interactions were taken to be Lennard-Jones potentials:

$$V_{LJ}(r) = 4\varepsilon\left[\left(\frac{\sigma}{r}\right)^{12} - \left(\frac{\sigma}{r}\right)^{6}\right] \quad (3)$$

where r is the interatomic distance, and ε and σ are the energy and length parameters, respectively.[17] The Lorentz−Berthelot combination rule[22] was used to obtain the Lennard-Jones parameters of the hetero atomic pairs. The S−Au pair interaction (chemisorptions) was modeled using the Morse potential:[23]

$$V_{Au-S}(r) = D_e \exp[-\alpha(r - r_e)]\{\exp[-\alpha(r - r_e)] - 2\} \quad (4)$$

where D_e and r_e are the well depth and distance at the minimum of the potential energy, respectively. The Lennard-Jones and Morse parameters were taken from previous simulations.[14,17,15]

Constant number, volume, and temperature (NVT) MD simulations were run using the Berendsen thermostat.[24] The equation of motion was integrated using the velocity Verlet algorithm with a time step of 1.0 fs. All gold atoms were fixed in position. The two-dimensional periodic boundary conditions with a minimum image convention[22] were applied using the lateral lattice vectors of 19.58 nm, 11.54 nm, 0 and 0, 23.07 nm, 0. The DL POLY package[25] was used to implement the MD methods described above.

The initial condition of the MD simulation was chosen as follows: the bulk SAM was first generated, in which the alkyl chains of the ODT molecules stand up and their S atoms form a $\sqrt{3} \times \sqrt{3}R30°$ overlayer on the gold (111) surface.[3] SAM patterns were then carved out from the bulk SAM. Each SAM pattern was relaxed by running a constant temperature MD simulation for 2 ns at 1 K. A NVT MD simulation was then run at 300 K for 10 ns or more. In this main simulation run, the temperature increased rapidly from zero to 300 K within 5 ps. Therefore, the present simulation emulates the change in the nanometer-wide SAM pattern, which initially has the packing structure of the bulk SAM.

III. RESULTS AND DISCUSSION

The SAM lines of 0.9, 1.3, 1.7, 2.2, and 2.6 nm in width, which correspond to the 3, 4, 5, 6, and 7 rows of aligned ODT molecules, respectively, were simulated. Each SAM line was taken to be infinite in length by applying the periodic boundary conditions. The width of a SAM line was defined as the average lateral (perpendicular to the direction of line propagation) distance between sulfur atoms located at the periphery of the line. Figure 2 shows snapshots of the SAM lines of 1.3 (left column) and 1.7 (right column) nm in width. In both SAM lines, the alkyl chains tilted almost 25° from the surface normal (see the top panels of Figure 2). The sulfur atoms of the 1.3 nm-wide line moved significantly away from their initial positions, particularly those at the periphery of the line. Consequently, the SAM line after 10 ns was not straight, and its periphery was rugged (middle left, Figure 2). In the SAM lines of 1.7 nm (middle right, Figure 2) or greater in width, the sulfur atoms did not move significantly, except jiggling around their initial positions (middle right, Figure 2). Occasionally, however, there were molecules that moved their sulfur atoms away from the periphery while their alkyl chains remained attached to the

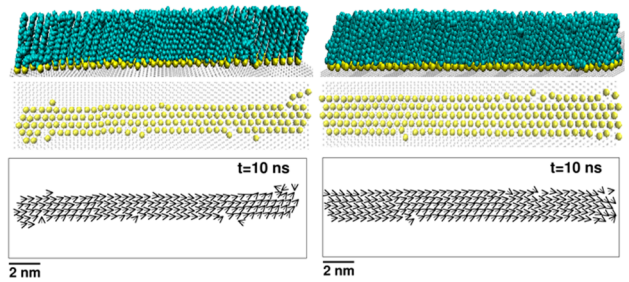

Figure 2. Snapshots of SAM lines with widths of 1.3 (left) and 1.7 (right) nm taken after 10 ns. Shown in the top panels are the side views of the SAM lines. In the middle panels, the bottom view of the SAM lines without the alkyl chains (dots represent the gold atoms) is shown. In the bottom, the tilt direction vector $\vec{v}_i$ for each molecule was drawn as an arrow.

dx.doi.org/10.1021/jp3099736 | J. Phys. Chem. C 2012, 116, 25928−25933

periphery. A molecule was also observed at the periphery, whose alkyl chain was laid down on the surface temporarily but stood upright almost immediately.

As shown in the bottom of Figure 2 (drawn are the tilt direction vectors $\vec{v}_i$ s), the alkyl chains tilted preferentially along the direction of line propagation for both 1.3 and 1.7 nm wide lines. Note, however, the $\vec{v}_i$ of each molecule slightly shifted to the right or left with respect to the direction of line propagation. This shifting constantly changed its direction left to right or vice versa with respect to the direction of line propagation, which is like a wagging motion of the chain (see below). In contrast, the $\vec{v}_i$'s of a circular SAM island rotated clockwise or counterclockwise around the center of the island.[15] This rotation in the tilt direction of the chain was attributed to the isotropy of a circular SAM pattern. The SAM does not have any preference in $\vec{v}_i$ provided that the tilt angle of chain θ_i is the same. In the case of a SAM line, however, the isotropy of the SAM pattern is broken, and the $\vec{v}_i$'s preferentially orient along the line direction to achieve the maximum interchain packing of molecules.

Figure 3 presents the mean azimuthal angle of $\vec{v}_i$'s, $\langle\varphi_i\rangle$, as a function of time for the SAM lines 1.3 (top), 1.7 (middle), and

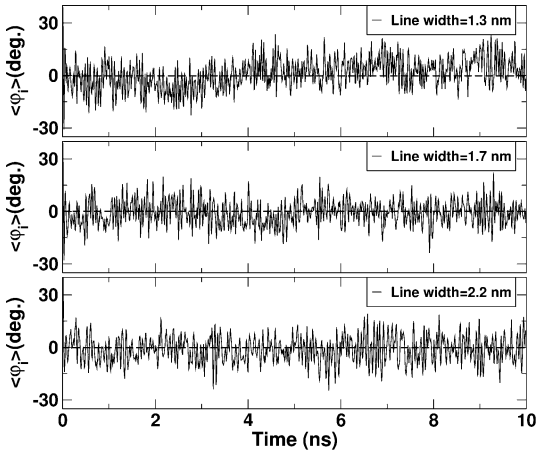

Figure 3. Wagging of the alkyl chains in a SAM line. The average tilt direction angle, $\langle\varphi_i\rangle$, was plotted as a function of time for the SAM lines of 1.3, 1.7, and 2.2 nm in width (solid line). The horizontal broken line, $\langle\varphi_i\rangle$ = 0, is drawn as a visual guide.

2.2 (bottom) nm in width. For the line propagating along the X axis, a negative (positive) $\langle\varphi_i\rangle$ value means the chains tilt left (right) with respect to the direction of line propagation. $\langle\varphi_i\rangle$ frequently alternates between a negative and positive value. This alternation in sign signifies the wagging of the alkyl chain with respect to the line direction. This wagging is small at times, in that $\langle\varphi_i\rangle$ oscillates without changing its sign. The average amplitude of the oscillation in $\langle\varphi_i\rangle$ for SAM lines of 1.3, 1.7, and 2.2 nm in width was 6.74°, 5.67°, and 6.16°, respectively.

A range of structural parameters of a SAM line was calculated by averaging over 800 snapshots taken for times ranging from 2 to 10 ns. For comparison, the bulk SAM values were drawn as horizontal broken lines. In Figure 4a, the average tilt angle of alkyl chains, $\langle\theta_i\rangle$, was plotted as a function of the line width (error bars represent the standard deviations). With increasing line width, $\langle\theta_i\rangle$ decreases and levels off at a width of 1.7 nm. Note that the tilt angles of the present SAM lines are smaller than the bulk SAM value (28.7°), except for the 0.9 nm-wide

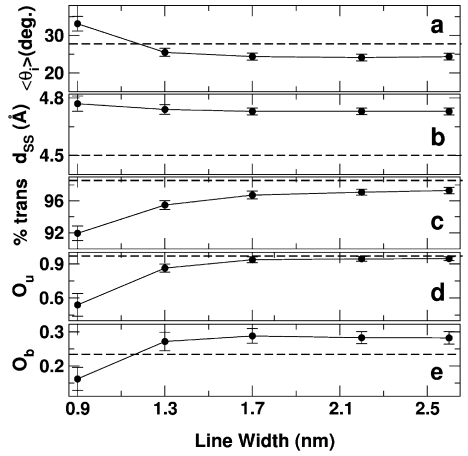

Figure 4. Molecular structure of a SAM line. Drawn are the average tilt angle $\langle\theta_i\rangle$ (a), the average neighboring sulfur−sulfur distance d_{SS} (b), the percentage of trans conformations in alkyl chains, % trans, (c), and the order parameters for the tilt direction O_u (d) and backbone orientation O_b (e) vectors versus the line width.

SAM line, which eventually becomes disconnected (see below). The tilt angles for the SAM lines of 1.3, 1.7, and 2.2 nm in width were 25.4°, 24.4°, and 24.1°, respectively.

The mean distance between neighboring sulfur−sulfur pairs, d_{SS}, was plotted as a function of the line width in Figure 4b. As the line broadened from 0.9 nm in width, d_{SS} decreased from 4.77 Å and leveled off to 4.73 Å at a line width of 1.7 nm. The converged d_{SS} value was greater than the bulk SAM value of 4.5 Å, indicating that the sulfur atom packing in this case was less compact. This reduced packing of sulfur atoms was attributed to ODT molecules at the periphery of the line, which has a lower number of nearest neighboring molecules than in the bulk SAM (which has six nearest neighbors).

The conformation of alkyl chain was also checked by counting the percentage of trans conformations (Figure 4c). With increasing line width, the trans percentage increased gradually from 91.9% and converged to a constant of 97.3% as the line width was increased from 0.9 to 2.6 nm. Note that the converged percentage of trans conformations is slightly lower than that of the bulk SAM.

In Figure 4d, the order parameter of the tilt direction, O_u, was plotted as a function of the line width. O_u increased and reached a plateau as the line width was increased from 0.9 nm. With the exception of the line width of 0.9 nm, O_u was close to 0.9, indicating that the tilt orientation of the alkyl chain was highly ordered (close to 1). O_u converged to the bulk SAM value at a line width of 2.6 nm, but the O_u value was very close to (within 3.9%) the bulk SAM value starting at a width of 1.7 nm.

The line width dependence of the backbone plane orientation was investigated by calculating O_b (Figure 4e). O_b increased from 0.15 to 0.25 with increasing line width, leveling off at a width of 1.7 nm. The O_b values were smaller than the corresponding O_u's, which range from 0.54 to 0.95. Therefore, the ordering in the backbone plane orientation $\vec{b}_i$ is not as complete as that of the tilt direction vector $\vec{u}_i$. Interestingly, the ordering of $\vec{b}_i$ for the SAM lines was actually greater than that of the bulk SAM. This was attributed to the preferential ordering of the tilt direction toward the direction of line propagation.

Overall, the various structural data shown in Figure 4 suggests that the SAM line stabilizes, and its structure

dx.doi.org/10.1021/jp3099736 | J. Phys. Chem. C 2012, 116, 25928−25933

resembles that of the bulk SAM as its width reaches 1.7 nm. This width presumably sets the ultimate resolution of the SAM lines. The present lower bound for the width of a stable SAM line is slightly smaller than the minimum width of a stable circular SAM island (= 1.9 nm).[15]

The SAM lines with a width <1.7 nm decomposed into smaller segments, which were slightly rounded and thicker than the original line (Figure 5). This decomposition was initiated

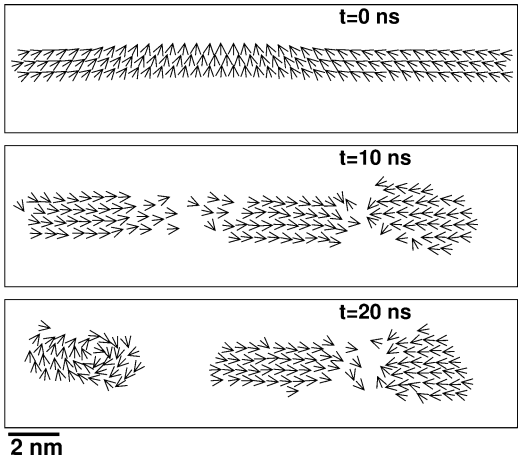

Figure 5. Disconnection of the SAM line. Shown are the tilt direction vectors $\vec{v}_i$'s (drawn as arrows) at times 0 (top), 10 (middle), and 20 ns (bottom) for the 0.9 nm wide SAM line. With time, the SAM line deforms and cleaves into segments. In this and all the following figures, a scale bar is drawn at the lower left corner.

by the mobile sulfur atoms located at the periphery of the line. These sulfur atoms deviated from their original positions due to thermal motion, making holes in the initially compactly packed line. Some of these deviated sulfur atoms did not move back to their original positions, making one portion of the line round and thick. The line is eventually broken as more molecules are drawn to this bulge (middle, Figure 5). In this process, some molecules at the peripheries of the segments tilted up to 38° from the surface normal. As the gap between the disconnected segments became larger, the molecules in each segment gradually recovered the original compact $\sqrt{3} \times \sqrt{3}R30°$ packing of the sulfur atoms and the approximately 24° tilt angle of the alkyl chain. The thiol molecules located at the edges of the broken lines repeated the folding and unfolding of their chains. After 20 ns, the fragmented line formed several SAM islands (bottom of Figure 5). Note that the alkyl chains tilted toward a different direction depending on which of the three SAM islands they belong to. The $\vec{v}_i$'s in the middle island tilted toward the right, whereas chains in the right island were tilted left. In the left island, which is almost circular in shape, $\vec{v}_i$'s rotated clockwise around the center of island. The $\vec{v}_i$'s in this island actually changed their direction clockwise to counterclockwise or vice versa with a period of 10s of ns. This periodic change in the rotation direction has also been found in a previous simulation of circular SAM islands.[15] The other two segments (middle and right) will eventually become circular in shape and show rotation in the $\vec{v}_i$'s.

In the above, infinitely long SAM lines were examined. SAM lines with a finite length were now investigated. Figure 6 presents the initial and final snapshots of SAM lines of 4 (top), 6 (second from top), 8 (second from bottom), and 10 (bottom) nm in length. The width of each line was 1.7 nm. The

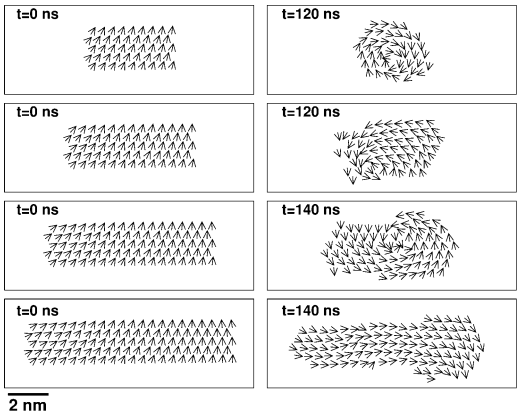

Figure 6. SAM lines with a finite length. 1.7 nm wide lines were simulated with lengths of 4 (top), 6 (second from top), 8 (second from bottom), and 10 (bottom) nm. Shown are the tilt direction vectos $\vec{v}_i$'s represented as arrows.

shortest SAM line (top) eventually became an almost circular island within 120 ns. The tilt direction of each molecule rotated clockwise around the center of the island (top right). Although not circular in shape, the SAM lines of 6 and 8 nm in length became severely deformed after 120 and 140 ns, respectively. In both SAM lines, the tilt direction $\vec{v}_i$ exhibited counterclockwise rotation around the center of the pattern, which is characteristic of a circular SAM island. Both patterns will further deform and become circular with time. The SAM line, 10 nm in length overall, maintained its linear shape, even after 140 ns. The tilt direction $\vec{v}_i$ was aligned along the direction of the propagation line but not as perfectly as in the infinite line with the same width. Note that the ends of the line are rounded. The right end of the line became thicker than its initial width. For the snapshot shown in the bottom right panel of Figure 6, the structural parameters shown in Figure 4 were calculated. The mean tilt angle of the alkyl chains, $\langle\theta_i\rangle$, was 22.41°, which was slightly lower than that of the infinite line (24.37°). The order parameters, O_u and O_b, for this line were 3.6% and 2.9%, respectively, lower than those of the infinite line with the same width. Therefore, the molecular orientation in this finite SAM line was less ordered. On the other hand, d_{SS} and % trans were similar to the corresponding values of the infinite line. Overall, a line with a finite length further destabilizes a SAM line in that the line becomes thicker, shorter, and rounder than its initial shape.

This study examined how close two parallel SAM lines can be without merging. This pertains to the best spatial resolution of the SAM patterns. Two parallel lines, 2.2 nm in width, were taken, and the interline spacing was varied: 2.3 (Figure 7a,b) and 2.9 (Figure 7c,d) nm. The spacing between the two lines was calculated from the nearest S−S distance of two adjacent lines. Initially, the sulfur atoms settled down at the 3-fold hollow sites of the gold surface to give a $\sqrt{3} \times \sqrt{3}R30°$ overlayer structure. The nearest distance between sulfur atoms belonging to two different lines was 2.31 nm. The length of the ODT molecule (in the coarse grained atom model) was calculated to be 2.28 nm at its all-trans conformation. A simple geometric consideration shows that, at 2.31 nm separation, two adjacent ODT molecules of two separate lines can touch each other if they tilt 24.9° toward each other. As shown in Figure 4a, the tilt angle of the chain for the 2.2 nm wide line was 24° on average with a standard deviation of 1°. Therefore, the

dx.doi.org/10.1021/jp3099736 | J. Phys. Chem. C 2012, 116, 25928−25933

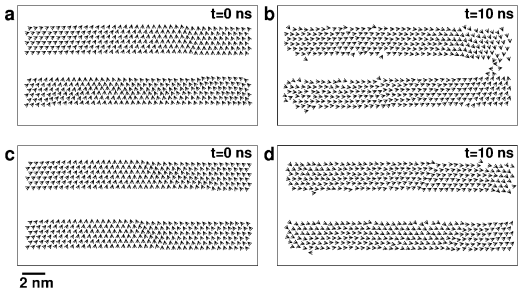

Figure 7. Minimum separation of two parallel lines. In the top and bottom panels, two lines (with the width of 2.2 nm) separated by 2.3 and 2.9 nm, respectively, were drawn. In each case, the snapshots taken at times, t, of 0 and 10 ns were plotted.

chains belonging to the two lines can touch each other if the fluctuation in the tilt angle from its average is considered. The $\vec{v}_i$'s drawn in Figure 7b show that few molecules are moving out from the original lines and bridge the lines. On the other hand, two SAM lines initially 2.9 nm apart did not coalescence. At this separation, the ODT molecules belonging to different lines can touch each other if they lie down on the surface. On the other hand, the interchain packing in each line prevents the molecules from tilting more than 30° from the surface normal. Therefore, two adjacent lines remain apart if their separation is ≥2.9 nm, and this probably sets the highest spatial resolution that can be achieved using the SAM lines of ODT. This minimum spacing will decrease (increase) if the SAM lines made from shorter (longer) alkyl chains are considered.

Having examined the properties of SAM lines above, nanopatterns made of SAM lines were then studied. As the crossing of lines commonly occurs in nanopatterns, cross patterns prepared from two SAM lines were simulated (Figure 8). The crossing of the two lines further destabilizes the SAM pattern: the lines, 0.9 (top) and 1.3 (middle) nm in width, give

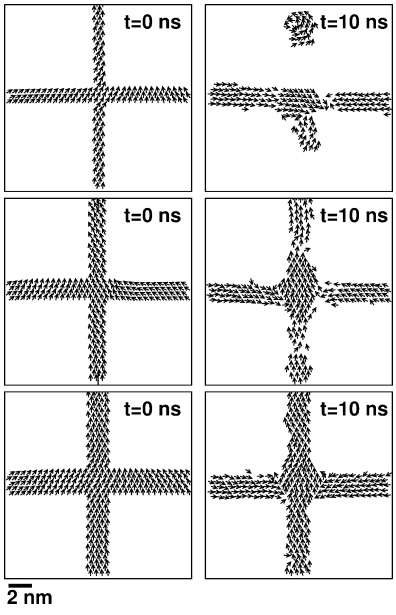

Figure 8. The cross patterns made from SAM lines. Shown are the snapshots of $\vec{v}_i$'s for the cross patterns made of SAM lines with widths of 0.9 (top), 1.3 (middle), and 1.7 nm (bottom). The left and right columns correspond to the snapshots at times, t, of 0 and 10 ns, respectively.

cross patterns that were eventually disconnected. Note that the infinitely long SAM line of 1.3 nm in width was not disconnected, as shown in Figure 2. In the case of a line width of 1.7 nm, the cross pattern maintained its original shape. The crossing point of the pattern became thicker than the original line width and round in shape to increase the interchain packing by pulling some molecules. Note that the $\vec{v}_i$'s generally point upward in a vertical line, whereas the $\vec{v}_i$'s belonging to the left and right portions of the horizontal line point right and left, respectively. The alignment of $\vec{v}_i$'s was not as complete as in a single infinite line. The order parameters, O_u and O_b, for the cross pattern shown in the bottom right of Figure 8 were 31% and 9.9% lower, respectively, than the corresponding values for the single line with the same width. The other structural parameters ($\langle\theta_i\rangle$, d_{SS}, and % trans) were virtually identical to those of the single line of 1.7 nm in width.

The L-shaped patterns of the SAM (Figure 9) were also simulated by varying the line width: 0.9 (top), 1.3 (middle),

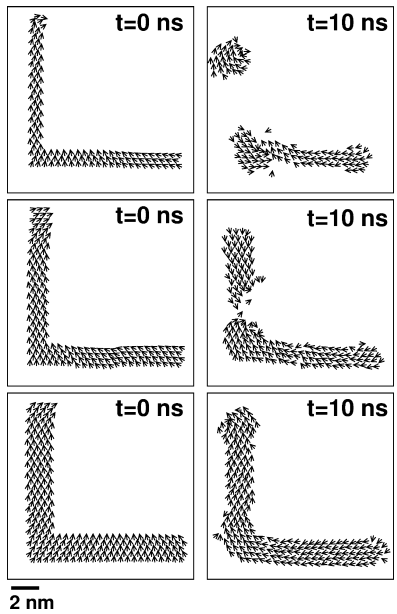

Figure 9. The L-shaped pattern made of SAM lines. Shown are the patterns made of 0.9 (top) 1.3 (middle), and 1.7 (bottom) nm wide SAM lines. In the left and right columns, the snapshots of $\vec{v}_i$'s taken at times, t, of 0 and 10 ns, respectively, were drawn.

and 1.7 nm (bottom). As in the cross patterns above, the L patterns made from the lines, 0.9 and 1.3 nm in width, were disconnected after 10 ns (see the top and middle panels). Both the finite length of lines and crossing of lines destabilize the patterns. The L shape of the pattern survived after 10 ns for the 1.7 nm wide line. The crossing point of the horizontal and vertical lines was rounded (bottom right). Note that the tilt direction vectors, $\vec{v}_i$, change smoothly from the left to upward as the line propagation changes from the horizontal to vertical direction. Regarding the cross patterns, $\vec{v}_i$'s were not as well aligned along the line direction as they are in an infinite line. Quantitatively, O_u, and O_b were 18% and 8.8% smaller than those of the single line with the same width. The values of $\langle\theta_i\rangle$, d_{SS}, and % trans of the patterns were similar to those of the single line.

dx.doi.org/10.1021/jp3099736 | J. Phys. Chem. C 2012, 116, 25928−25933

IV. CONCLUSIONS

MD simulations were used to examine the molecular details of the nanometer-wide SAM lines of ODT deposited on gold. The compact and well-defined molecular packing found in the bulk SAM persisted for line patterns as narrow as 1.7 nm in width. This sets the theoretical minimum width of a SAM line. Some differences were observed compared to the bulk SAM: the alkyl chains of the molecules stood more upright and were tilted preferentially along the line propagation with small wagging motion. The packing of sulfur atoms was less compact, but the backbone orientation of the alkyl chain was more ordered. If the line width is less than 1.7 nm, a SAM line deformed its shape or cleaved into segments. The minimum separation between the two adjacent lines was 2.9 nm, which sets the ultimate spatial resolution of the SAM lines. A SAM line with a finite length became more unstable, thicker, and shorter than the infinite line with the same width. Crossing of the SAM lines further destabilized the SAM pattern.

AUTHOR INFORMATION

Corresponding Author

*E-mail: jkjang@pusan.ac.kr.

Notes

The authors declare no competing financial interest.

ACKNOWLEDGMENTS

This study was supported by National Research Foundation Grants funded by the Korean Government (MEST) (No. 2011-0027696 and No. 2011-0027445). J.J. wishes to thank the Korea Institute of Science and Technology Information for allowing him the use of the PLSI supercomputing resources.

REFERENCES

(1) Schreiber, F. *Prog. Surf. Sci.* **2000**, *65*, 151−257.
(2) Love, J. C.; Estroff, L. A.; Kriebel, J. K.; Nuzzo, R. G.; Whitesides, G. M. *Chem. Rev.* **2005**, *105*, 1103−1170.
(3) Ulman, A. *Chem. Rev.* **1996**, *96*, 1533−1554.
(4) Woodruff, D. P.; Delchar, T. A. *Modern Techniques of Surface Science*; Cambridge University Press: New York, 1986.
(5) Ginger, D. S.; Zhang, H.; Mirkin, C. A. *Angew. Chem., Int. Ed.* **2004**, *43*, 30−45.
(6) Mirkin, C. A. *ACS Nano* **2007**, *1*, 79−83.
(7) Jeon, N. L.; Nuzzo, R. G.; Xia, Y.; Mrksich, M.; Whitesides, G. M. *Langmuir* **1995**, *11*, 3024−3026.
(8) Aizenberg, J.; Black, A. J.; Whitesides, G. M. *Nature* **1999**, *398*, 495−498.
(9) Xu, S.; Miller, S.; Laibinis, P. E.; Liu, G.-y. *Langmuir* **1999**, *15*, 7244−7251.
(10) Mooney, J. F.; Hunt, A. J.; McIntosh, J. R.; Liberko, C. A.; Walba, D. M.; Rogers, C. T. *Proc. Natl. Acad. Sci.* **1996**, *93*, 12287−12291.
(11) Ressier, L.; Martin, C.; Viallet, B.; Grisolia, J.; Peyrade, J.-P. *J. Vac. Sci. Technol. B* **2007**, *25*, 17−20.
(12) Turchanin, A.; Schnietz, M.; El-Desawy, M.; Solak, H. H.; David, C.; Gölzhäuser, A. *Small* **2007**, *3*, 2114−2119.
(13) Hong, S.; Mirkin, C. A. *Science* **2000**, *288*, 1808−1811.
(14) Ahn, Y.; Saha, J. K.; Schatz, G. C.; Jang, J. *J. Phys. Chem. C* **2011**, *115*, 10668−10674.
(15) Saha, J. K.; Ahn, Y.; Kim, H.; Schatz, G. C.; Jang, J. *J. Phys. Chem. C* **2011**, *115*, 13193−13199.
(16) Ghorai, P. K.; Glotzer, S. C. *J. Phys. Chem. C* **2007**, *111*, 15857−15862.
(17) Hautman, J.; Klein, M. L. *J. Chem. Phys.* **1989**, *91*, 4994−5001.
(18) Bhatia, R.; Garrison, B. J. *Langmuir* **1997**, *13*, 4038−4043.
(19) Fujiwara, S.; Sato, T. *J. Chem. Phys.* **1999**, *110*, 9757−9764.
(20) Jorgensen, W. L.; Maxwell, D. S.; Tirado-Rives, J. *J. Am. Chem. Soc.* **1996**, *118*, 11225−11236.
(21) Jorgensen, W. L.; Madura, J. D.; Swenson., C. J. *J. Am. Chem. Soc.* **1984**, *106*, 6638−6646.
(22) Allen, M. P.; Tildesley, D. J. *Computer Simulation of Liquids*; Oxford University Press: New York, 1987.
(23) Zhao, X.; Leng, Y.; Cummings, P. T. *Langmuir* **2006**, *22*, 4116−4124.
(24) Berendsen, H. J. C.; Postma, J. P. M.; van Gunsteren, W. F.; DiNola, A.; Haak, J. R. *J. Chem. Phys.* **1984**, *81*, 3684−3690.
(25) Smith, W.; Yong, C. W.; Rodger, P. M. *Mol. Simul.* **2002**, *28*, 385−471.